Synthesis and Structure of *trans*-$[O_2(Im)_4Tc]Cl \cdot 2H_2O$, *trans*-$[O_2(1\text{-meIm})_4Tc]Cl \cdot 3H_2O$ and Related Compounds

P. H. FACKLER, M. J. LINDSAY, M. J. CLARKE*

Department of Chemistry, Boston College, Chestnut Hill, Mass. 02167, U.S.A.

and M. E. KASTNER

Department of Chemistry, Boston University, Boston, Mass. 02215, U.S.A.

Received July 23, 1984

Abstract

The synthesis, spectra and HPLC behavior of a series of *trans*-dioxotechnetium(V) complexes with imidazole and bidentate nitrogen ligands are reported. Crystals of *trans*-$[O_2(Im)_4Tc]Cl \cdot 2H_2O$ were found to form in the monoclinic space group $C2/c$ with unit cell parameters a = 13.249 (3) Å, b = 11.239 (2) Å, c = 14.358 (3) Å and β = 115.56 (2)°. The cell volume is 1929 (1) Å^3 with Z = 4. The similar compound *trans*-$[O_2(1\text{-meIm})_4Tc]Cl \cdot 3H_2O$ crystallized in the same space group with a = 20.980 (5) Å, b = 8.599 (3) Å, c = 16.105 (3) Å and β = 124.22 (2)°. The cell volume is 2402 (1) Å^3 with Z = 4. The unweighted R-factors for the two structures are 0.091 and 0.122, respectively. The Tc=O and Tc–N bond distances are essentially identical in the two structures and are 1.71 Å and 2.15 Å, respectively. The imidazole ligands are canted slightly by an average angle of 15° off a plane perpendicular to that of the technetium and nitrogens. Infrared absorbances assigned to the asymmetric O=Tc=O stretch occur in the range 810–830 cm^{-1}. The compounds are all diamagnetic due to the strong tetragonal distortion exerted by the oxo ligands. Proton NMR resonances are deshielded slightly relative to the free ligands. The imidazole complexes are unstable in aqueous solution and the bidentate amine complexes are unstable at low pH. HPLC capacity factors by reverse-phase ion-pair chromatography varied in an unexpected manner and, in general, decreased with increasing aliphatic chain length of the eluant anion.

Introduction

The interactions of technetium ions with biologically important compounds are of considerable importance owing to the widespread use of ^{99m}Tc in diagnostic radio-imaging. The technetium (III) through (V) oxidation states predominate in aqueous media in the presence of mild reductants [1–7] and so are also prominent in radiopharmaceutical preparations and *in vivo* [3–5]. Complexes of technetium in these oxidation states with amine and imine ligands are of interest as models for the binding of technetium ions to amino acids, proteins, nucleotides and chromatin material. In general, Tc(V) tends to form complexes of the general type *trans*-$[O_2L_4Tc]^+$, where L is a nitrogen ligand. While no complexes of this kind have been prepared with mono-amine ligands, complexes with pyridines are stable in nonaqueous media [8] and complexes with chelating amines persist in water for varying lengths of time [9].

Since imidazole rings on purines and histidine are often involved in metal ion coordination in biological systems, an investigation of the complexation of imidazole with the *trans*-dioxotechnetium(V) core was undertaken in an effort to explore the structure and stability of such ions. Similarly, chelation of Tc(V) by proximal amine sites on proteins seems a likely mode of binding this metal ion and the elucidation of the structure and spectroscopic properties of bidentate amine complexes of *trans*-$[O_2Tc]^+$ is a prerequisite to identifying these species in biological or radiopharmaceutical systems. Abbreviations used: DACH, 1,2-diaminocyclohexane; RR-DACH, 1,2-(–), R,R-diaminocyclohexane; en, 1,2-diaminoethane; 1,2-DAP, 1,2-diaminopropane; 1,3-DAP, 1,3-diaminopropane; Im, imidazole; meIm, methylimidazole.

Experimental

Synthesis

Imidazole complexes were prepared by placing 185 mg (0.37 mmol) of [n-Bu_4N][OCl_4Tc] [10] and 200 mg (2.94 mmol) of imidazole (8:1 ligand/Tc ratios were used for 1-meIm and 4-meIm) in an Erlenmeyer flask and then adding 20 mL of absolute ethanol with constant stirring. The mixture was stirred for 5 min while an orange color developed and

*Author to whom correspondence should be addressed.

0020-1693/85/$3.30

the resulting solution was rotary evaporated to yield an orange oil, which was redissolved in a mixture of 30 mL acetone and 1 mL water. Following a second rotary evaporation, 30 mL of acetone was poured onto the resulting pink solid, which was then suspended by vigorously scraping off the sides of the vessel. The suspension was filtered and the solid washed with an additional 50 mL of acetone to remove any unreacted ligand. The final pink solid was obtained in 90–95% yield. Crystallization was accomplished by dissolution of the solid in absolute ethanol followed by slow evaporation. Complexes with diamine chelates, *trans*-$[O_2L_2Tc]Cl$ where L = en, 1,2-DAP, 1,3-DAP, 1,2-DACH and 1,2-RR-DACH, could be prepared by the following methods:

Method A

Approximately 150 mg of $[n\text{-}Bu_4N][OCl_4Tc]$ was dissolved in a minimum of tetrahydrofuran (THF) and 5–7 drops of the ligand added until the green color of the starting material disappeared. On standing a brownish-orange to pink aggregate formed, which was removed by filtration and washed with THF. The residue was dissolved in a minimum amount of water and charged onto a Sephadex CM C-25 cation exchange column, which was eluted with water followed by 0.05 M ammonium formate (pH 6.6). The desired complex eluted as an orange-pink band, which was subjected to repeated rotary-evaporation (with occasional addition of water) until the buffer was entirely removed. Following dissolution of the filtrate in a minimum amount of water and filtration, a few drops of a saturated solution of $(n\text{-}Bu_4N)Cl$ (NaI in the case of the 1,2-DAP complex) was added. The final orange crystalline products formed upon overnight diffusion of ethanol into the mixture. Yields: en, 79% (needles); 1,3-DAP, 68% (needles); 1,2-DAP, 90% (amorphous); DACH, 80% (microcrystalline) and RR-DACH, 60% (microcrystalline).

Method B

A modification of Method A allowed NH_4TcO_4 to be used directly as the starting material. Approximately 20 mg of NH_4TcO_4 was dissolved in a minimum of concentrated HCl and allowed to stand for 15 minutes before rotary-evaporating the solution to dryness. The residue was then dissolved in a minimum volume of a THF/ethanol (2:1 v/v) mixture and 3-5 drops of the ligand added. The resulting brownish-orange to pink flocculent precipitate which formed was removed by filtration and washed with THF, before final isolation as in Method A. Yields: en, 45%; 1,3-DAP, 60% and DACH, 39%.

Method C

Approximately 20 mg of NH_4TcO_4 was dissolved in a minimum amount of water. Several drops of the ligand were then dispersed in an equal volume of water to which was added a three-fold molar quantity (60 mg) of sodium dithionite. This mixture was then combined with the pertechnetate solution. These reaction mixtures typically turned a brown color after 1–2 min and finally to an orange-pink solution on standing overnight. The solution was then subjected to ion exchange chromatography and products isolated as above. Yields: en, 51%; 1,2-DAP, 70%; 1,3-DAP, 66%; DACH, 20% and RR-DACH, 17%. **Caution!** All syntheses were performed with ^{99}Tc, which is a β-emitting isotope with a half-life of 2.15×10^5 yrs. Precautions for handling this material are described elsewhere [2–9].

Compound Characterization

The elemental analyses (except for ^{99}Tc) summarized in Table I were performed by the Stanford Microanalytical Laboratory, Stanford, CA. Technetium analyses were performed by dissolving known quantities of the compound in 8 mL of acetone and adding approximately 2 mL of a 30% solution of H_2O_2 to oxidize the metal to TcO_4^-. Calibration standards were similarly prepared by dissolving $(NH_4)TcO_4$, which had been recrystallized from 0.1 M ammonia with the addition of a few drops of H_2O_2, and then dried at 25° in a vacuum desiccator for 10 hrs. Aliquots of 25–125 μL were then combined with 10 mL of Fischer Scintiverse SO-X-I scintillation cocktail and Tc determinations made on an LKB-1217 or Nuclear Chicago Unilux II scintillation counter. Counting was done for 60 sec over a ^3H window with 10^4–10^5 counts usually being obtained for samples and standards. Unknown samples were determined using a linear least squares fit to the standards.

Infrared spectra were taken on a Perkin-Elmer Model 599B grating spectrophotometer in CsI pellets. UV-visible spectra were obtained on a Perkin-Elmer Model 575 spectrometer equipped with a digital background corrector and a thermostatted sample cell. The decomposition of *trans*-$[O_2(en)_2Tc]^+$ was monitored spectrophotometrically at 23° by following the change in absorbance at 313 nm over at least 5 half lives. Absorbance data over time was collected via an interface to a Polymorphic 8812 microcomputer and treated by a linear least squares method [11]. PMR spectra were recorded on a Varian FT-80A Fourier transform spectrometer. Magnetic susceptibility measurements were made on a Cahn Model 7500 Electrobalance equipped with a 14,502 G permanent magnet. All spectra were recorded at room temperature.

HPLC

Various types of reverse phase ion pair chromatography were employed to separate the various complexes. Separations were performed on a Laboratory

TABLE I. Elemental Analyses[a] for *trans*-$[O_2Tc]^+$ Complexes with Amine and Imine Ligands.

Ligand	Waters of Solvation	Element	Calcd	Found
Im	2	C	30.36	30.23
		H	4.25	4.22
		N	23.60	23.63
		Cl	7.5	8.5
		Tc	20.8	20.5
1-meIm	3	C	35.01	35.85
		H	5.51	5.60
		N	20.42	20.89
		Cl	6.46	6.97
		Tc	18.0	17.6
4-meIm	2	C	36.20	36.37
		H	5.51	5.60
		N	20.42	20.89
		Cl	6.46	6.97
		Tc	18.0	17.6
DACH	2	C	33.68	33.46
		H	7.50	7.08
		N	13.01	12.83
		Cl	8.23	8.27
		Tc	22.98	22.2
(RR)DACH	2	C	33.45	33.87
		H	7.50	7.21
		N	13.01	12.73
		Cl	8.23	7.45
		Tc	22.98	21.9
1,2-DAP	1	C	16.99	17.30
		H	5.24	5.06
		N	13.21	13.00
		I	29.93	29.45
		Tc	23.3	22.6
1,3-DAP	1.5	C	21.09	21.09
		H	6.80	6.28
		N	16.40	16.24
		Cl	10.37	10.47
		Tc	28.9	27.6

[a] Im = imidazole, DACH = 1,2-diaminocyclohexane, DAP = diaminopropane.

Data Control chromatograph equipped with three LDC Constametric III pumps, a LDC UV III Monitor set at 254 nm, a Rheodyne 7161 injection port and a Waters μ-Bondapak octadecylsilane column at a flow rate of 2.0 mL/min. The eluents used were 0.2 M solutions of the ammonium salts of formic, acetic and propionic acids; methylaminium formate, -acetate and propionate; and ethyaminium formate, -acetate and -propionate adjusted to pH 7.0. All eluents were filtered through a 0.45 μm Millipore filter before use. Samples were filtered through a Swinney type filter containing a Gelman thick glass fiber filter (pore sizes 0.2 to 10 μm) prior to injection.

Structure Determination of trans-$[O_2(Im)_4Tc]Cl\cdot 2H_2O$

Intensity data were measured on an automated diffractometer with background counts collected at the extremes of the scan for one-half the time of the scan. Three standard reflections were measured every 50 reflections during the course of the measurements.

The structure was solved by standard heavy atoms techniques [12] with the Tc ion being determined to be located at a center of symmetry at (1/4, 1/4, 0) from a Patterson map. All non-hydrogen atoms were found in a series of difference Fourier maps. The water molecule is described as half atoms disordered about the center of symmetry at (0, 0, 0). The chloride is assigned to a general location, and given half weight to balance charge. The final model used anisotropic thermal parameters for all non-hydrogen atoms, and calculated positions for the four hydrogens in the plane of each imidazole ring (C–H = 0.95 Å, B(H) = B(C) = 1.0 Å^2) were included in subsequent refinement cycles as fixed contributers. The structure was refined by full-matrix least-square methods [13]. The final data/parameter ratio was 6.3. A final difference Fourier synthesis was judged to be free of significant features.

Crystallographic data for both structures are summarized in Table II. Final values of atomic coordinates in the asymmetric unit cell of *trans*-$[O_2(Im)_4Tc]Cl\cdot 2H_2O$ are given in Table III. The final calculated and observed structure amplitudes (×10) and a listing of thermal factors are available in Tables Is and IIIs, respectively, in the supplementary material.

Structure Determination of trans-$[O_2(1\text{-}meIm)_4Tc]Cl\cdot 3H_2O$

Intensity data were measured as indicated for the previous structure. Data were collected as the triclinic cell, with cell constants of 11.337 (5) Å, 14.062 (7) Å, 8.599 (5) Å, 107.74 (4)°, 112.29 (4)° and 88.79 (4)° and then transformed to the monoclinic, C centered cell reported here by using the transformations: $h_{C2/c} = 2h + l$, $k_{C2/c} = l$ and $l_{C2/c} = -(h + k + l)$. Duplicate reflections were averaged, and the structure solved by direct methods [14]. Since the space group is not uniquely determined by the systematic extinctions, both *Cc* and *C*2/*c* are both possible. Attempts to solve the structure in the acentric space group *Cc* failed. The solution in *C*2/*c* is reported. (Data on another crystal had originally been collected as a triclinic cell with cell constants of 8.685 (2), 8.688 (2), and 14.106 (3) Å and 73.72 (2), 103.56 (2), and 80.615 (2)°. When solved in the centric space group $P\bar{1}$, with two half molecules in the asymmetric unit, the structure clearly showed the presence of a glide plane. Using a new crystal the mirror plane perpendicular to b was evident in an axial photograph and data was collected in the monoclinic system). It cannot presently be determined whether the

TABLE II. Crystallographic Data for *trans*-$[O_2(Im)_4Tc]Cl \cdot 2H_2O$ and *trans*-$[O_2(1\text{-meIm})_4Tc]Cl \cdot 3H_2O$.

	trans-$[O_2(Im)_4Tc]Cl \cdot 2H_2O$	*trans*-$[O_2(1\text{-meIm})_4Tc]Cl \cdot 3H_2O$
Formula	$H_{20}C_{12}N_8O_4ClTc$	$H_{28}C_{16}N_8O_4ClTc$
Fw	474.7	530.8
Crystal Dimensions	0.1 × 0.2 × 0.5	0.5 × 0.67 × 0.37
Color	pink	red
Radiation Source (Cu K_α) λ (Å)	1.5418	1.5418
Diffractometer	Syntex $P2_1$	Syntex $P2_1$
Space Group	*C*2/*c*	*C*2/*c*
Cell constants (*a*, *b*, *c*), Å	13.249 (3)	20.980 (5)
	11.239 (2)	8.599 (3)
	14.358 (3)	16.105 (3)
Cell constants (β), °	115.56 (2)	124.22 (2)
Cell volume, $Å^3$	1929 (1)	2402 (1)
Z (fw/unit cell)	4	4
d (calcd.), g/cm^3	1.63	1.47
d (obs.), g/cm^3	1.64	1.54
Total no. of observations	1187	2630
Observed Reflections[a]	759	1144
Scan mode	$\theta-2\theta$	$\theta-2\theta$
$2-\theta$ range, °	3–100	3–100
Scan width above and below K_α	0.7	0.5
Scan rate, °/min	2–12	2–12
No. of variables in least squares	119	139
$R = \Sigma(\|F_0\| - \|F_c\|)/\Sigma\|F_0\|$	0.091	0.122
$R_w = [\Sigma w(\|F_0\| - \|F_c\|)^2/\Sigma\|w(F_0)^2\|]^{1/2}$	0.112	0.149

[a] Reflections with $F_0 > 3\sigma(F_0)$ were retained as observed and used in the solution and refinement of the structure.

TABLE III. Atomic Coordinates in the Unit Cell of *trans*-$[O_2(Im)_4Tc]Cl \cdot 2H_2O$.

Atom Type	Coordinates[a]		
	x	*y*	*z*
Tc	1/4	1/4	0
Cl	0.082 (1)	0.159 (1)	0.380 (1)
O2	0.008 (3)	0.020 (3)	0.043 (2)
O	0.357 (1)	0.346 (1)	0.018 (1)
N1	0.372 (2)	0.110 (1)	0.062 (1)
N2	0.440 (2)	−0.072 (2)	0.097 (2)
N3	0.268 (2)	0.292 (2)	0.152 (2)
N4	0.324 (2)	0.373 (2)	0.305 (2)
C1	0.347 (2)	−0.005 (2)	0.054 (2)
C2	0.527 (3)	0.009 (3)	0.138 (3)
C3	0.482 (2)	0.123 (3)	0.114 (2)
C4	0.335 (2)	0.375 (2)	0.216 (2)
C5	0.249 (2)	0.282 (2)	0.295 (2)
C6	0.221 (2)	0.226 (2)	0.204 (2)

[a] The numbers in parentheses are the estimated standard deviations.

disappointing quality of the final structure is due to a misassignment of space group, the low data/parameter ratio inherent in centered systems, microscopic twinning not observable under polarized light, unresolvable disorder of the imidazole resulting in interchange of C2 and N2 on the imidazole or other problems.

The Tc cation is located at a center of symmetry at (0, 0, 0) as is the chloride anion at (1/4, 1/4, 1/2). Peaks appropriate for hydrogen atoms were found in difference maps for the ring atoms, but the methyl hydrogens were not well defined. The final model used anisotropic thermal parameters for all non-hydrogen atoms, and calculated positions for the three hydrogens in the plane of each imidazole ring (C–H = 0.95 Å, B(H) = B(C) = 1.0 $Å^2$) were included in subsequent refinement cycles as fixed contributers. The six hydrogens on the methyl groups were not included in the calculations. The structure was refined by full-matrix least-square methods [13]. The final data/parameter ratio was 8.2. A final difference Fourier synthesis was judged to be free of significant features.

Final values of atomic coordinates in the asymmetric unit of the unit cell of *trans*-$[O_2(1\text{-meIm})_4Tc]Cl \cdot 3H_2O$ are given in Table IV. The final calculated and observed structure amplitudes (×10) and a listing of thermal factors are available in Tables IIs and IVs, respectively, in the supplementary material.

Results

Spectra

Reference to the infrared spectra for the complexes summarized in Table V shows that the asymmetric

TABLE IV. Atomic Coordinates in the Unit Cell of *trans*-$[O_2(1\text{-meIm})_4Tc]Cl\cdot 3H_2O$.

Atom Type	Coordinates[a]		
	x	*y*	*z*
Tc	0	0	0
Cl	1/4	1/4	1/2
O	0.032 (1)	−0.149 (2)	−0.038 (1)
O2	0.068 (2)	0.314 (2)	0.352 (2)
N1	0.043 (1)	0.160 (3)	−0.060 (1)
N2	0.110 (2)	0.264 (2)	−0.112 (2)
N3	0.106 (1)	0.019 (2)	0.146 (1)
N4	0.227 (2)	0.007 (2)	0.270 (2)
C1	0.099 (2)	0.131 (3)	−0.076 (2)
C2	0.024 (1)	0.305 (3)	−0.080 (2)
C3	0.064 (1)	0.375 (3)	−0.110 (1)
C4	0.168 (2)	0.305 (4)	−0.143 (3)
C5	0.180 (1)	−0.044 (3)	0.169 (2)
C6	0.119 (1)	0.081 (3)	0.223 (2)
C7	0.192 (1)	0.079 (3)	0.302 (2)
C8	0.320 (1)	−0.042 (4)	0.339 (3)

[a]The numbers in parentheses are the estimated standard deviations.

stretching frequencies of the O=Tc=O group occur at somewhat lower energy for the imidazole complexes than for the diamine chelates, but that all lie in the region 810–830 cm^{-1} [9–15]. Tc–N stretches also occur at significantly lower energies for the imidazole complexes, while the energies of the TcO_2 bending modes [16] lie approximately in the same region for all compounds. The broad electronic absorptions in the 480–500 nm region listed in Table VI lend these complexes an orange to pink color and vary somewhat with the nitrogen ligand, while the bands at 305–317 nm vary little with the nitrogen ligand. Absorbances around 245 nm in the imidazole complexes are due to ligand π–π^* transitions. The PMR spectral lines listed in Table VII for the imidazole

TABLE VI. Wavelength Maxima[a] for the Electronic Spectra of *trans*-$[O_2L_4Tc]^+$.

Ligand	λ_{max}	ϵ (M^{-1} cm^{-1})
Im	213	1.76×10^4
	245	6.15×10^3
	317	9.10×10^2
	484	1.28×10^2
1-meIm	214	1.60×10^4
	246	5.60×10^3
	317	9.45×10^2
	489	1.38×10^2
4-meIm	218	1.77×10^4
	246	5.82×10^3
	316	6.51×10^2
	483	9.52×10^2
4-Aminopyridine[a]	209	3.69×10^4
	250	4.32×10^4
	262	3.96×10^4
	305	5.86×10^3
	522	3.00×10^2
en[b]	233	8.08×10^3
	313	5.31×10^2
	490	2.65×10^1
1,2-DAP	230	7.47×10^3
	314	2.27×10^2
	494	1.11×10^1
1,3-DAP	230(sh)	$\simeq 8 \times 10^3$
	313	5.87×10^2
	489	5.76×10^1
DACH	232	7.90×10^3
	314	5.83×10^2
	495	2.49×10^1
(RR)DACH	233(sh)	$\simeq 8 \times 10^3$
	313	5.11×10^2
	496	4.21×10^1

[a]Taken from ref. [8]. [b]Taken from ref. [9].

TABLE V. Infrared Stretching Frequencies of *trans*-$[O_2L_4Tc]^+$.

Ligands	Infrared Frequencies (cm^{-1})				
	$\delta(NH_2)$	$\gamma(NH_2)$	$\nu_{asym}(TcO_2)$	ν(Tc–N)	$\delta(TcO_2)$
Imidazole			810(s)	319(w)	277(m)
1-MeIm			812(s)	313(w)	254(m)
4-MeIm			810(s)	327(w)	260(m)
Pyr[a]			828(s)		
en[b]	1585(s)	1055(s)	835(vs)	420(w)	285(m)
1,2-DAP	1585(s)	1040(m)	825(vs)	414(w)	275(w)
1,3-DAP	1575(s)	1055(s)	818(vs)	425(w)	290(m)
DACH	1580(s)	1060(s)	830(vs)	430(w)	265(w)
(RR)DACH	1585(s)	1060(s)	830(vs)	430(w)	265(w)

[a]Taken from ref. [8]. [b]Taken from ref. [9].

TABLE VII. PMR Data[a] for *trans*-$[O_2L_4Tc]^+$ in d_4-methanol.

Ligand	Assignment	δ[a] (ppm)	Number of Protons	Number of Peaks in Multiplet	$^3J_{H-H}$(Hz)	Shift Rel. to Free Ligand
Imidazole	H(2)	8.00	1	1		0.23
	H(5)	7.21	1	1		0.15
	H(4)	7.29	1	1		0.07
1-Methylimidazole	H(2)	7.92	1	1		0.42
	H(4, 5)	7.17	2	2		0.24
	CH_3	3.73	3	1		0.12
4-Methylimidazole	H(2)	7.76	1	1		0.39
	H(5)	6.88	1	1		0.23
	CH_3	2.17	3	1		0.04
en[b]	H(1, 2)	3.07	4	5		0.84
1,2-DAP	H(2)	3.23	1	1		0.51
	H(1)	2.25	2	2	5	0.14
	CH_3	1.39	3	2	8	0.45
1,3-DAP	H(1)	3.11	4	3	6	0.58
	H(2)	1.95	2	5	5	0.50
c						

[a]Positions are given relative to tetramethylsilane at 37°. [b]Taken from ref. [9]. [c]NMR's of DACH complexes were not possible owing to low solubility.

complexes are shifted 0.23–0.42 ppm downfield for the C(2) protons, 0.15–0.24 ppm for C(5) protons and 0.07–0.24 for C(4) protons. Protons on a methyl group attached to a nitrogen are shifted slightly more downfield than those on a C(4) methyl. PMR shifts of diamine complexes were 0.5–0.84 ppm downfield relative to the free ligand for α-protons and 0.14 for the β-protons in 1,2-DAP. All compounds were found to be diamagnetic by the Faraday method as is typical for *trans*-dioxo complexes of Tc(V) and Re(V) [7].

Stability

None of the complexes exhibited oxidation or reduction processes by cyclic voltammetry. However, attempts to reduce *trans*-$[O_2(en)_2Tc]^+$ over zinc amalgam in N_2 purged solutions of 1 M HCl yielded a green solution after 40 h, which eluted with 3 M HCl from a Dowex-50 cation exchange column. Rotary evaporation produced an unstable, lime-green solid. Infrared analysis showed the absence of the asymmetric [O=Tc=O] stretch and retention of the amine and C–N vibrations. New, strongly absorbing bands at 325 and 350 cm^{-1} were attributed to Tc–Cl stretches.

The imidazole complexes were unstable in aqueous solution and appeared to rapidly decompose to the purple-brown $[TcO_2]_n \cdot H_2O$. Upon lowering the pH from 8 to 6 in the presence of excess imidazole the band at 484 nm shifted to approximately 455 nm and increased in intensity. However, upon lowering the pH to 2.2 this band disappeared and was replaced by a broad, lower intensity band at 375 nm. The ethylenediamine complex underwent a fairly rapid acid-catalyzed hydrolysis to an uncharacterized yellow material (λ_{max} = 245, 290(sh), 450, 500(sh)), which remained in solution and appeared to be stable at low pH, and a light brown precipitate. The relative stability of the chelates in aqueous media was: 1,2-DAP ~ en > DACH > 1,3-DAP. The observed first-order rate constant for the decay of *trans*-$[O_2(en)_2Tc]^+$ was estimated to be $5.4 \pm 0.1 \times 10^{-3}$ sec^{-1} at pH 3.88. However, PMR of this complex revealed ligand dissociation to be taking place even at pH 7, so that it is likely that there are both proton dependent and proton independent pathways. The net absorbance changes that could be observed below pH 2 and above pH 6 were fairly small. At the low pH extreme it is likely that the reaction of interest was nearly complete before it could be observed by conventional mixing and spectrophotometric techniques. However, at the high pH range the reaction observed spectrophotometrically was over long before the hydrolysis was judged to be complete by NMR techniques. In an effort to increase the stability, purity and crystallinity of the DACH species, pure 1,2-(–),R,R-diaminocyclohexane was employed as a ligand; however, this made little difference in the observed properties.

Chromatography

While the diamine chelates were stable upon ion exchange chromatographic separation at neutral pH,

the imidazole complexes decomposed fairly quickly. HPLC analysis of most of the diamine chelate complexes could be accomplished using 0.2 M solutions of ammonium carboxylates at pH 7 as the eluant with the complexes eluting as broad, tailing peaks. An exception to this was the DACH complex, which was strongly retained but eluted slowly with 0.2 M ethylaminium propionate in purely aqueous media. Best results for this complex were obtained with 0.2 M ammonium carboxylate eluants containing 20% methanol. Use of methylaminium or ethylaminium ions in place of ammonium improved the chromatographic characteristics somewhat. The chromatographic behavior of these complexes with varying eluants was often the opposite of that expected [17]. In general, increasing the chain length of the carboxylate anion (from formate to propionate) decreased the retention times of most complexes and decreased column efficiency of the column [18] as measured by the number of theoretical plates determined by the 5σ method†. Increasing the chain length of the amine cation normally increased the retention time and column efficiency with formate and acetate anions but caused the reverse to occur with propionate.

Structure of trans-[$O_2(Im)_4Tc$]Cl·2H_2O

Figure 1 is a computer-drawn [19] model of the cation of *trans*-[$O_2(Im)_4Tc$]$^+$. Tables VIII and IX give the individual bond distances and angles in *trans*-[$O_2(Im)_4Tc$]$^+$. The cation is a distorted octahedron, with a Tc=O bond distance of 1.71 (2) Å and a Tc–N bond distance of 2.15 (2) Å. The imidazole rings are twisted slightly away from the O=Tc=O axis. For the rings associated with N1 and N2, the dihedral angles between the imidazole ring and the Tc–N equatorial plane are 75° and 82°, respectively. The rings are 88° from one another.

The water molecule of solvation is hydrogen bonded to the oxygen (02–01, 2.7 Å). The water

†$N = 25\ (t_r - t_o)/w_{4.4}$, where N = number of height equivalent theoretical plates, t_r = retention time, t_o = column dead time and $w_{4.4}$ = peak width at 4.4% of the peak height.

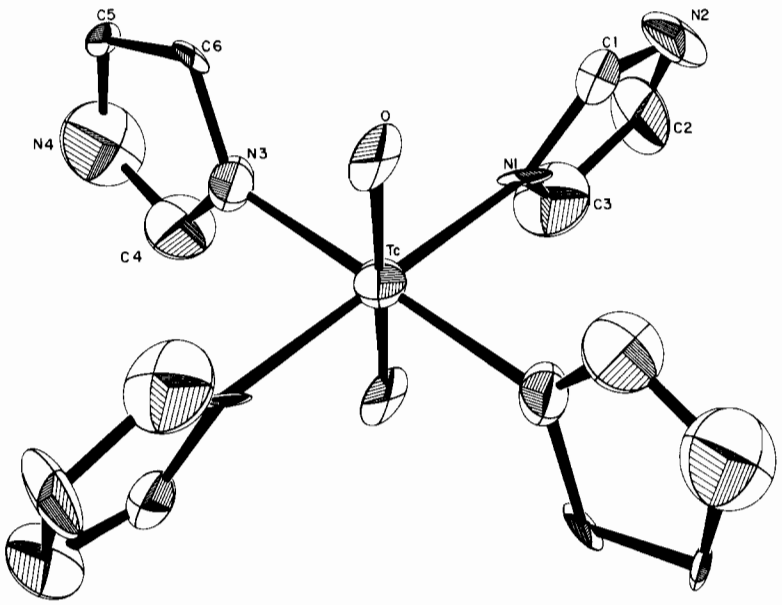

Fig. 1. ORTEP diagram of *trans*-[$O_2(Im)_4Tc$]$^+$: thermal ellipsoids are drawn at 50% probability.

TABLE VIII. Bond Distances in the Unit Cell of *trans*-[$O_2(Im)_4Tc$]Cl·2H_2O.

Bond Type	Distance Å	Bond Type	Distance Å	Bond Type	Distance Å
Tc–O	1.71 (2)	N2–C1	1.35 (3)	N4–C4	1.34 (5)
Tc–N1	2.15 (2)	N2–C2	1.39 (4)	N4–C5	1.40 (4)
Tc–N3	2.15 (2)	N3–C4	1.34 (3)	C2–C3	1.39 (4)
N1–C1	1.33 (3)	N3–C6	1.38 (4)	C5–C6	1.35 (3)
N1–C3	1.33 (3)				

[a] The numbers in parentheses are the estimated standard deviations.

TABLE IX. Bond Angles in the Unit Cell of *trans*-$[O_2(Im)_4Tc]Cl \cdot 2H_2O$.

Bond Type	Angle Degree	Bond Type	Angle Degree	Bond Type	Angle Degree
O–Tc–N1	89 (1)	C4–N4–C5	106 (2)	N3–C6–C5	106 (2)
O–Tc–N3	89 (1)	N1–C1–N2	111 (2)	C1–N1–Tc	124 (2)
N3–Tc–N1	90 (1)	N2–C2–C3	108 (3)	C3–N1–Tc	127 (2)
C1–N1–C3	109 (2)	N1–C3–C2	107 (2)	C4–N3–Tc	126 (2)
C1–N2–C2	105 (2)	N3–C4–N4	109 (3)	C6–N3–Tc	124 (1)
C4–N3–C6	109 (2)	N4–C5–C6	109 (2)		

[a] The numbers in parentheses are the estimated standard deviations in the last significant figure.

TABLE X. Bond Distances in the Unit Cell of *trans*-$[O_2(1\text{-meIm})_4Tc]Cl \cdot 3H_2O$.

Bond Type	Distance Å	Bond Type	Distance Å	Bond Type	Distance Å
Tc–O	1.71 (2)	N2–C1	1.36 (4)	N4–C5	1.41 (4)
Tc–N1	2.14 (2)	N2–C3	1.36 (4)	N4–C7	1.28 (4)
Tc–N3	2.15 (2)	N2–C4	1.60 (6)	N4–C8	1.66 (4)
N1–C1	1.36 (5)	N3–C5	1.48 (4)	C2–C3	1.32 (5)
N1–C2	1.29 (5)	N3–C6	1.24 (4)	C6–C7	1.34 (3)

[a] The numbers in parentheses are the estimated standard deviations.

molecule is also close to the chloride anion (O2–Cl, 2.5 Å; 02–Cl′, 3.5 Å) and to N4 (N4–O2, 2.87 Å). The chloride also makes close contact with N2 (Cl–N2, 3.07 Å), and C5 (Cl–C5, 3.25 Å). Other nonbonded contacts are greater than 3.5 Å. The assignments of the 3 and 4 positions on the imidazole ring (N4 and C5) were made on the basis of the close contact of N4 to O2. Assignment of N2 and C2 was made on the basis of the Cl–N2 contact.

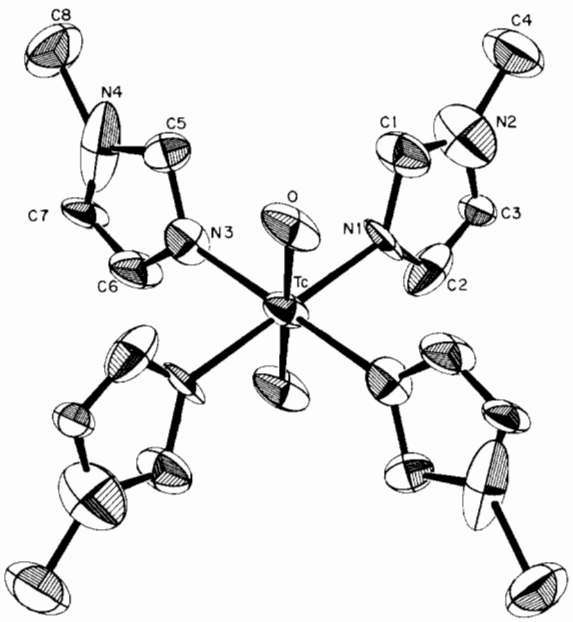

Fig. 2. ORTEP diagram of *trans*-$[O_2(1\text{-meIm})_4Tc]^+$: thermal ellipsoids are drawn at 50% probability.

Structure of trans-[O_2(1-meIm)$_4$Tc]Cl·3H_2O

Figure 2 is a computer-drawn [19] model of *trans*-$[O_2(1\text{-meIm})_4Tc]^+$. Tables X and XI give the individual bond distances and angles in the technetium cations. The cation is a distorted octahedron with Tc=O at 1.71 (2) and a Tc–N bond distance of 2.14 (2) Å. The imidazole rings are twisted off the perpendicular to the N–Tc–N plane and make dihedral angles with the Tc–N equatorial plane of 75° and 69° for the two rings associated with N1 and N2, respectively. These rings are 88° from each other.

The water molecule of solvation is hydrogen bonded to the oxygen (02–0, 2.7 Å). The water molecule is also close to the chloride anion (O2–Cl, 3.22 Å) and to C3 (C3–O2, 2.76 Å) and is 2.90 Å from a symmetry related self. The chlorine also makes close contact with C7 (Cl–C7, 3.07 Å).

Discussion

Synthesis and Stability

It is probably significant that the originally orange product changes to the pink, crystalline material isolated following dissolution in wet acetone. Simple substitution of the imidazole ligands onto $[n\text{-}Bu_4N][OCl_4Tc]$ would be expected to result in $[O(Im)_4Tc]^{3+}$

TABLE XI. Bond Angles in the Unit Cell of *trans*-$[O_2(1\text{-meIm})_4Tc]Cl\cdot 3H_2O$.

Bond Type	Angle Degree	Bond Type	Angle Degree	Bond Type	Angle Degree
O–Tc–N1	88 (1)	C5–N3–C6	107 (2)	N4–C5–N3	98 (3)
O–Tc–N3	94 (1)	C5–N4–C7	116 (2)	N3–C6–C7	116 (3)
N1–Tc–N3	90 (1)	C5–N4–C8	119 (3)	N4–C7–C6	103 (3)
C1–N1–C2	107 (3)	C7–N4–C8	125 (3)	C2–N1–Tc	126 (2)
C1–N2–C3	107 (3)	N1–C1–N2	107 (3)	C1–N1–Tc	126 (2)
C1–N2–C4	132 (3)	N1–C2–C3	112 (3)	C6–N3–Tc	129 (2)
C3–N2–C4	121 (2)	N2–C3–C2	106 (2)	C5–N3–Tc	123 (2)

[a] The numbers in parentheses are the estimated standard deviations in the last significant figure.

or a similar, deprotonated species and attack by water probably provides the additional oxygen necessary to complete the *trans*-dioxotechnetium(V) core. Indeed, the recent structure determination of *cis*-$[OCl(quin)_2Tc]$ [20], where quin = 2-methyl-8-quinoline, suggests that ligand attack occurs at the open site, which is labilized by the *trans*-oxo ligand, followed by ligand rearrangement to displace the equatorial halides. The structures of *trans*-$[O(OH_2)(acac_2en)Tc]^+$ [21], where $acac_2en$ = N,N′-ethylenebis(acetylacetone imine), and $[O(CH_3CH_2O)Br_2(4\text{-nitropyridine})_2Tc^V]$ [22] are also consistent with the final step being solvent attack *trans* to the oxo and subsequent deprotonation to yield either the *trans*-dioxotechnetium(V) core, in the case of water addition, or *trans*-$[O{=}Tc{-}OR]^{2+}$, in the case of an alcohol solvent.

Several methods of synthesizing the diamine chelates were employed in order to devise techniques of preparing these directly from $[^{99m}TcO_4]^-$, which is the universal starting material for technetium radiopharmaceuticals. Simple HCl treatment of the pertechnetate ion prior to addition of the ligand (Method B) should result in the formation of $[OCl_4Tc]^-$, so that this provides a rapid, simple, single-reaction-vessel means of achieving these complexes. Reduction of pertechnetate by a large excess of dithionite in the presence of the ligand (Method C) also provides a direct route from pertechnetate; however, the long times required for the reaction to go to completion limits is utility in radiopharmacy due to the relatively short half-life (6 h) of ^{99m}Tc.

The diamine chelate complexes were considerably more stable in water than the imidazole species and maintained their integrity for sufficiently long periods under approximately physiological conditions to be used in radiodiagnostic preparations. Among the chelated complexes, the steric strain resulting from the six-membered ring formed on technetium coordination with 1,3-DAP caused this complex to be significantly less stable than the five-membered ring complexes. The less flexible DACH ligands formed somewhat less stable complexes than the ethylenediamine and 1,2-DAP ligands. The instability of the imidazole complexes in aqueous media suggests that stable monodentate coordination of the $[O{=}Tc{=}O]^+$ core is unlikely in biological systems; however, chelation by proximal histidinyl imidazoles or adjacent purines on nucleic acids should yield fairly stable species. Similarly, amine chelation of oxotechnetium(V) cores by proteins should hold the metal ion fixed for sufficiently long periods to be useful in radioscintigraphy.

The hydrolysis studies of the ethylenediamine complex clearly show the lability of this ligand in acidic media; however, this appears to be more complicated than a single pseudo first order reaction. One process yields a stable yellow material, which remains in solution, and the other ends in the formation of a precipitate, which is likely $[TcO_2]\cdot xH_2O$. Moreover, biphasic behavior was evident in the absorption traces around pH 4 suggesting subsequent, slower reactions of these materials. Acid hydrolysis of the imidazole complexes also resulted in a solution-stable, yellow complex, whose spectrum was similar to, but distinct from that formed from the diamine chelates. While these species were not characterized, the differences in their spectra suggest that they retain some of the nitrogen ligand.

Structure

Figures 1 and 2 reveal the tetragonally distorted octahedral structure which is now typical for Tc(V) coordinated by amine or imine ligands [8–9]. While the Tc=O bond distances of 1.71 Å are slightly shorter than the average bond length of 1.74 (2) Å found in analogous complexes [8], the difference is within experimental error. The Tc–N bond distances are identical with the average of 2.15 (1) Å found in other similar compounds [8, 9]. The average tilt of the imidazole rings from the O=Tc=O axis (~15°) is very similar to that seen for pyridine rings in *trans*-$[O_2(t\text{-BuPyr})_4Tc]F_3CSO_3\cdot H_2O$ and is probably due to packing forces [9].

Spectra

The metal–oxygen infrared stretching frequencies listed in Table V are substantially less than those

observed in mono-oxotechnetium(V) complexes (940–980 cm^{-1}), which involve partial triple bonding [8, 22], and fall well within the expected range (790–835 cm^{-1}) for the asymmetric O=M(V)=O stretch, where M = Tc or Re [23]. The slight downfield PMR shifts are probably due to a combination of electron-withdrawing effects induced by the $[O=Tc=O]^+$ core and the diamagnetic anisotropy resulting from the circulation of π-electrons around the tetragonal axis, which is fairly strong in the case of the $[O=Tc-OR]^{2+}$ core [22].

The strong tetragonal distortion of the ligand field resulting from the oxo ligands causes the d_{xy} orbital to lie substantially below the degenerate set of d_{xz} and d_{yz} orbitals. This leads to a pairing of the valence electrons in this d^2 ion to yield a diamagnetic, $^1A_1$ ground state (assuming C_{4v} site symmetry). Ligand field transitions for the ethylenediamine complex have been reported as: 793 nm, $^1A_1$ (b_2^2) → ^1E (b_2e), $\epsilon \simeq 2$ M^{-1} cm^{-1}; 598 nm, $^1A_1 \rightarrow {}^1A_2$ (b_2b_1), $\epsilon \simeq 2$ M^{-1} cm^{-1}; and 490 nm ($^1A_1 \rightarrow {}^1B_2$ (b_2a_1), $\epsilon \simeq 20$ M^{-1} cm^{-1}) [24]. Ligand field parameters are: Δ = 18,700 cm^{-1}, δ_{b_2-e} = 16,100 cm^{-1} and $\delta_{b_1-a_1}$ = 5,900 cm^{-1}. Assuming these assignments to be correct, the bands occurring between 480 and 500 nm can be attributed to the $^1A_1 \rightarrow {}^1B_2$ transition. Since the more intense, higher energy bands around 315 nm are relatively insensitive to the nitrogen ligand, these may involve oxygen to Tc(V) charge transfer transitions.

HPLC

Chromatographic separations by reverse-phase ion-pairing chromatography yielded capacity factors which varied in an unexpected manner. In this type of chromatography, increasing the aliphatic chain-length of the counter ion generally increases the capacity factor (retention time) for the analyte ion, owing to the increased lipophilic character of the ion pair. Similarly, column efficiency is increased since the counter ions themselves are better able to bind to the organic coating and so tend to cover any polar, silanol sites on the bare packing material. Increasing the chain length of the eluant ion of like charge with the analyte usually increases the competition for column binding and so decreases retention time of the analyte, while column efficiency is usually increased due to better coverage of polar sites. The long tailing peaks and inverted retention behavior observed with the diamine chelate complexes with increasing organic character of the eluant anions suggests that polar interactions with underivatized sites on the column are important in their chromatographic retention. The increase in retention time observed with increasing cation chain length further indicates the importance of polar interactions, which probably result from hydrogen binding between the oxo ligands and open silanol groups, while the simultaneous increase in column efficiency also suggests a degree of separation due to lipophilic interactions. The relatively greater organic character of the DACH complex causes it to behave normally with varying cation chain length. Finally, considering the decomposition behavior of these complexes, it is possible that some of the chromatographic peak tailing is due to sample decomposition on the column.

Acknowledgements

This work was supported by PHS Grants CA24344 and GM26390 and a grant from the American Cancer Society (Massachusetts Division).

Supplementary Material

Temperature factors for nonhydrogen atoms, calculated and observed and structure factor amplitudes for *trans*-$[O_2(Im)_4Tc]Cl \cdot 2H_2O$ and *trans*-$[O_2(1\text{-meIm})_4Tc]Cl \cdot 3H_2O$, and complete listings of infrared spectra. Ordering information given on any current masthead page.

References

1 A. Davison and A. G. Jones, *Int. J. Appl. Radiat. Isot., 33,* 875 (1982) and other articles in this issue.
2 K. Schwochau, *Radiochem. Acta, 32,* 139 (1983).
3 E. Deutsch, K. Libson, S. Jurisson and L. Lindoy, *Prog. Inorg. Chem., 30* (1983), in press.
4 W. C. Eckelman and W. A. Volkert, *Int. J. Appl. Radiat. Isot., 33,* 945 (1982).
5 S. C. Srivastava and P. Richards, in G. V. S. Rayudu, (ed.), 'Radiotracers for Medical Applications', CRC Press, Boca Raton, Fla. 1981, p. 107.
6 G. Bandoli, U. Mazzi, E. Roncari and E. Deutsch, *Coord. Chem. Rev., 44,* 191 (1982).
7 M. J. Clarke and P. H. Fackler, *Struct. and Bonding, 50,* 57 (1982).
8 M. E. Kastner, P. H. Fackler, M. J. Clarke and E. Deutsch, *Inorg. Chem., 23* (1984) in press.
9 M. E. Kastner, M. J. Lindsay and M. J. Clarke, *Inorg. Chem., 21,* 2037 (1982).
10 F. A. Cotton, A. Davison, V. W. Day, L. D. Gage and H. S. Trop, *Inorg. Chem., 18,* 3024 (1979).
11 J. W. Moore and R. G. Pearson, 'Kinetics and Mechanism, 3rd edn', Wiley, New York, 1981, p. 70.
12 C. R. Hubbard, C. O. Quicksall and R. A. Jacobson, 'The Fast Fourier Algorithm and Report Is-2625', Ames Laboratory, Iowa State University, Ames, Iowa, 1971.
13 R. L. Lapp and R. A. Jacobson, 'ALLS', A Generalized Crystallographic Least Squares Program, National Technical Information Service #IS-4708 UC-4, Springfield, Va, 1979.
14 P. Main, 'Multan 78', Department of Physics, University of York, York, England.
15 A. G. Jones, B. V. DePamphilis and A. Davison, *Inorg. Chem., 20,* 2037 (1981).
16 M. Baluka, J. Hanuza and B. Jeżowska-Trzebiatowska, *Bull. Acad. Pol. Sci., Ser. Sci. Chim., 20,* 271 (1971).

17 R. Gloor and E. L. Johnson, *J. Chromat. Sci., 15,* 413 (1977).
18 'Technical Bulletin #102', Waters Assoc., Milford, Mass.
19 C. K. Johnson, 'ORTEP', A Fortran Thermal Ellipsoid Plot Program (ORNL-3794), Oak Ridge Natl. Laboratory, Oak Ridge, Tenn., 1965.
20 E. Deutsch, B. E. Wilcox and M. J. Heeg, submitted for publication.
21 S. Jurrison, L. F. Lindoy, K. P. Dancey, M. McPartlin, P. A. Tasker, D. K. Uppal and E. Deutsch, *Inorg. Chem.,* (1984), in press.
22 P. H. Fackler, M. E. Kastner and M. J. Clarke, *Inorg. Chem., 23* (1984) in press.
23 B. Jeżowska-Trzebiatowska and J. Hanuza, *J. Mol. Struct., 19,* 109 (1973).
24 M. Baluka, J. Hanuza and B. Jeżowska-Trzebiatowska, *Bull. Acad. Pol. Sci., Ser. Sci. Chim., 20,* 271 (1972).